SPACE-TIME RESOLVED DIAGNOSTICS OF RADIO FREQUENCY GLOW DISCHARGE KINETICS

R. Gottscho

▶ **To cite this version:**

R. Gottscho. SPACE-TIME RESOLVED DIAGNOSTICS OF RADIO FREQUENCY GLOW DISCHARGE KINETICS. Journal de Physique Colloques, 1987, 48 (C7), pp.C7-693-C7-699. 10.1051/jphyscol:19877172 . jpa-00226996

HAL Id: jpa-00226996
https://hal.science/jpa-00226996

Submitted on 4 Feb 2008

HAL is a multi-disciplinary open access archive for the deposit and dissemination of scientific research documents, whether they are published or not. The documents may come from teaching and research institutions in France or abroad, or from public or private research centers.

L'archive ouverte pluridisciplinaire **HAL**, est destinée au dépôt et à la diffusion de documents scientifiques de niveau recherche, publiés ou non, émanant des établissements d'enseignement et de recherche français ou étrangers, des laboratoires publics ou privés.

JOURNAL DE PHYSIQUE
Colloque C7, supplément au n°12, Tome 48, décembre 1987

SPACE-TIME RESOLVED DIAGNOSTICS OF RADIO FREQUENCY GLOW DISCHARGE KINETICS

R.A. GOTTSCHO

AT and T Bell Laboratories, Murray Hill, NJ 07974, U.S.A.

ABSTRACT

Three applications of space-time resolved spectroscopy to the study of plasma processes are reviewed briefly. Each application emphasizes a different aspect of plasma chemistry: heterogeneous reactions, homogeneous reactions, and charged-particle transport. Spatially-resolved concentration profiles of reactants near surfaces provide estimates for heterogeneous reaction rates. This is demonstrated using data for CF_2 molecules near Si and O atoms near Al, graphite, and kapton. Space-time resolved plasma-induced emission is used to distinguish between dissociative excitation mechanisms in BCl_3-Ar discharge mixtures, where superelastic collisions of cold electrons with Ar metastables are shown to be important. Stark-mixed laser-induced fluorescence is used to measure the self-consistent electric fields that are responsible for controlling charged particle transport to and from device surfaces. The low frequency fields breathe periodically as they extract ions from the sheath.

I. INTRODUCTION

Current methods for fabricating microelectronic devices use plasma exposure to etch and deposit thin films for primarily two reasons: (1) electron-impact processes drive "high temperature" chemistry while avoiding the deleterious effects of high temperatures; and, (2) ion-impact processes lead to anisotropic heterogeneous reaction rates that are necessary for achieving larger scale integration. Although there are many successful applications of plasma chemistry, most processes now in use were developed empirically because of the difficulty in describing the non-equilibrium, non-linear interactions that occur in partially ionized gases.

The development of reliable plasma models will certainly help improve processing control and provide a more rational basis for process design. With such models, new device structures and new materials may be fabricated without time-consuming empirical development. However, the generation of reliable plasma models requires a close liaison with experiment. Non-intrusive, *in situ* diagnostic methods are needed to both test the results of model calculations and provide input for semi-empirical simulations.

In this talk, I will outline three sets of experiments where space-time resolved laser-induced fluorescence (LIF) and plasma-induced emission (PIE) spectroscopy have helped to elucidate important kinetic mechanisms in radio frequency glow discharges. The first experiments show how spatially-resolved, time-averaged LIF measurements of reactant densities near surfaces are used to obtain information on surface loss probabilities [1,2]. The second set of experiments illustrates the utility of space-time resolved diagnostics in determining the dominant mechanisms for formation of excited states in discharges through gas mixtures [3]. The last example shows how Stark-mixed LIF can be used to map out the space-time dependent fields in rf glow discharges [4,5]. The fields are of paramount

Article published online by EDP Sciences and available at http://dx.doi.org/10.1051/jphyscol:19877172

importance in controlling the transport of charged particles to device surfaces and enhancing (or sometimes diminishing) the rate of heterogeneous reactions.

II. EQUATION OF CONTINUITY

For each of the experiments, the results are analyzed using the one-dimensional equation of continuity that expresses conservation of density:

$$\frac{\partial n}{\partial t} = F(x,t) - L(x,t) - \frac{\partial \Gamma}{\partial x} \qquad (1)$$

where n is the density (cm^{-3}), F(x,t) and L(x,t) are the space-time dependent formation and loss functions ($cm^{-3}s^{-1}$), respectively, and Γ is the particle flux ($cm^{-2}s^{-1}$) along the x direction, which is taken to be perpendicular to the electrode surfaces in a parallel plate reactor. Radial gradients are ignored because the high 3-dimensional resolution of LIF has been exploited in measuring concentrations and fields along only the x direction.

III. REACTANT DEPLETION AT SURFACES

Consider the time-averaged atomic or molecular density near a surface downstream from a discharge source. If both homogeneous formation and loss processes are negligible, the flux to the surface is conserved and given by the rate of diffusion:

$$\frac{\partial \Gamma}{\partial x} = \frac{\partial}{\partial x}\left(D\frac{\partial n}{\partial x}\right) = 0 \qquad (2)$$

where D is the diffusion coefficient. The flux to the surface must be balanced by the net loss (or generation) rate at the surface [1]:

$$\lim_{x \to surf} D\frac{\partial n}{\partial x} = \frac{1}{4}\alpha \bar{v} n(x) \qquad (3)$$

where α is the loss probability at the surface and $\bar{v}$ is the thermal velocity. This boundary condition is used to solve Eq. (2) and obtain an expression for the density near the surface [1]:

$$n(x) = n_s\left[\frac{3\alpha x}{4\lambda} + 1\right] \qquad (4)$$

where n_s is the density at the surface (x=0) and $\lambda \approx D/3\bar{v}$ is the mean free path.

Using spatially-resolved LIF, the densities of reactants can be measured near surfaces and the net loss probability α can be estimated. This has been shown for the case of CF_2 molecules near a Si wafer downstream from a discharge through CF_4 [1]. The data in Ref. 1 show that the CF_2 density varies linearly with distance near the surface in accord with the simple prediction of Eq. 4. The vibrational dependence of the loss rate is readily obtained by tuning the laser to excite transitions from either the (0,0,0) or (0,1,0) levels of the $^1A_1$ ground state. The loss rate for the excited vibrational level is found to be roughly twice that for the ground vibrational level [1]. This may result from a faster reaction rate with the surface (either etching or deposition) or could simply reflect the rate of vibrational relaxation. Further experiments are necessary to resolve this ambiguity.

In a similar set of experiments, Selwyn [2] used two-photon laser-induced fluorescence to measure the concentrations of O atoms near graphite, aluminum, and kapton surfaces. Because these experiments were performed *in situ*, neither F(x,t) nor L(x,t) can be neglected. However, the diffusive term near the surface will often dominate the homogeneous formation and loss terms and, at least qualitatively, relative reactivities can be determined from the spatial concentration profiles. The data in Ref. 2 clearly show depletion of O atoms above the graphite-covered half of an aluminum electrode in an oxygen plasma: O atoms passivate aluminum but etch graphite. The effects of dc bias voltage on kapton etch rates in an oxygen plasma are also clear from the data in Ref. 2. Increasing the dc bias voltage results in increased O-atom depletion near kapton surfaces. This is consistent with ion-enhanced etching of kapton.

IV. EXCITATION KINETICS IN DISCHARGES THROUGH GAS MIXTURES

Although the reason a particular recipe works is often obscure, discharges through gas mixtures are used in many plasma applications. One difficulty in trying to unravel the chemistry of discharges through gas mixtures is the multitude of possible excitation and dissociation pathways. For example, in discharges containing rare gases, dissociation and excitation of molecules may occur by electron-impact, ion-impact, or metastable energy transfer. However, by making time-resolved density measurements, these mechanisms can be distinguished [3,6].

For example, consider dissociative excitation of BCl_3 to form short-lived BCl ($A\ ^1\Pi$) by hot electrons in the center of a low frequency discharge:

$$BCl_3 + e^- \rightarrow BCl(A^1\Pi) + 2Cl + e^- \tag{5}$$

In this case, the formation function is approximately in phase with the applied voltage and modulated at twice the fundamental frequency [3,6]:

$$F(x=0,t) \approx F_0 \sin^2 \omega t, \tag{6}$$

where ω is the frequency of the applied voltage used to drive the discharge and F_0 is the formation rate amplitude in the discharge center. For radiative decay, the loss rate is given by:

$$L(x=0,t) = n/\tau, \tag{7}$$

where $\tau = 19$ns is the BCl ($A^1\Pi$) lifetime. For $1/\tau \gg D/\Lambda^2$, where Λ is the characteristic diffusion length, the solution to Eq. 1 is simply [3,6]

$$n(t) = \frac{F_0}{\tau} \sin^2 \omega t. \tag{8}$$

The short-lived state density is in phase with the applied voltage and modulated at twice the fundamental frequency. Fig. 1 shows that emission from BCl ($A\ ^1\Pi$) in a 50 kHz discharge through neat BCl_3 approximately exhibits the time dependence expressed by Eq. 8.

When Ar is added to a low frequency discharge through BCl_3, the BCl $A^1\Pi$ emission intensity in the plasma center increases by more than an order of magnitude over a narrow concentration range (Fig. 2). Is this change a result of an increase in the hot electron-impact dissociative excitation rate (Eq. 5) or of some new process associated with Ar

metastables, Ar_m? Two metastable processes can be considered. The first is *direct* dissociative energy transfer:

$$Ar_m + BCl_3 \rightarrow Ar + BCl(A^1\Pi) + 2Cl \quad (9)$$

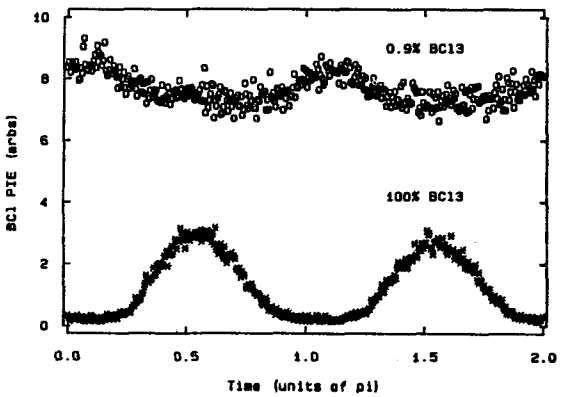

Fig. 1: Time-resolved BCl $(A^1\Pi)$ emission from the center of discharges containing BCl_3. The "*" points were obtained from a neat BCl_3 plasma and the "o" points from 0.9% BCl_3 in Ar. (From Ref. 3) Time in units of π refers to the phase of the applied voltage.

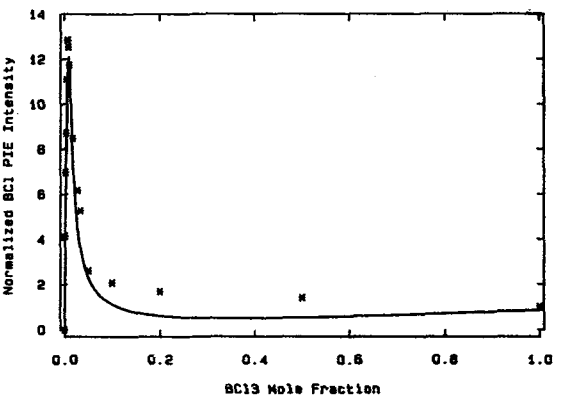

Fig. 2: Time-averaged BCl $(A^1\Pi)$ emission from the plasma center vs. BCl_3 mole fraction. The points were obtained experimentally and the solid curve is a fit to a model that includes the effects of superelastic electron collisions with Ar metastables. (From Ref. 3)

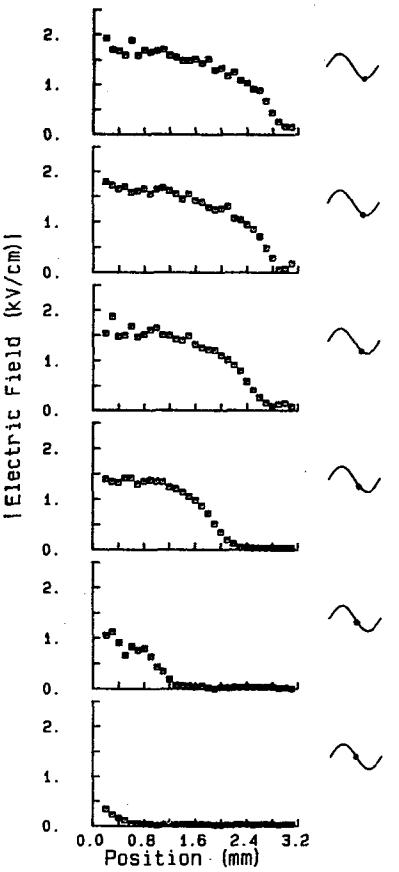

Fig. 3: Space-time resolved electric fields for first quarter of cathodic half-cycle of 30W, 50 kHz discharge through 5% BCl_3 in Ar. (From Ref. 5) Only the sheath fields are shown; the plasma center is at 8mm from the electrode at 0mm.

The second is *indirect* dissociative excitation by **hot** electrons created by superelastic collisions of cold electrons with Ar_m [3]:

$$Ar_m + e^-(\epsilon) \rightarrow Ar + e^-(\epsilon + 11.5eV) \quad (10a)$$

$$BCl_3 + e^-(\epsilon + 11.5eV) \rightarrow BCl(A^1\Pi) + 2Cl + e^- \quad (10b)$$

where $e^-(\epsilon)$ denotes a low energy electron. The rates for both Eq. 9 and 10 will be weakly modulated for frequencies above 50 kHz because neither the Ar_m nor the $e^-(\epsilon)$ densities are modulated on this time scale [3]. Therefore, if these mechanisms are important, the formation function will be approximately constant,

$$F(x=0,t) \approx S_0 \tag{11}$$

where S_0 represents the net formation rate by the slow processes in Eqs. 9 and 10. Substituting Eq. 11 into Eq. 1 and neglecting diffusion, the BCl ($A^1\Pi$) density is found to be approximately constant,

$$n \approx S_0/\tau. \tag{12}$$

As Fig. 1 shows, the BCl ($A^1\Pi$) density is weakly modulated, in accord with Eq. 12, under the same conditions that cause the overall increase in emission intensity (Fig. 2). The two slow mechanisms in Eqs. 9 and 10 can be distinguished by examining spatially-resolved PIE and LIF profiles as well as the functional form for the emission enhancement shown in Fig. 2. The details of this analysis can be found in Ref. 3, where the superelastic mechanism (Eq. 10) is found to be most important. The solid curve in Fig. 2 is a fit of the data to a model including superelastic effects.

V. SPACE-TIME RESOLVED ELECTRIC FIELDS AND ION TRANSPORT

Recently, a number of techniques have been used to measure sheath electric fields in glow discharges [4,5,7-9]. These measurements are crucially important in developing models for plasma processes because the self-consistent fields control ion and electron transport to and from device surfaces.

Consider the equation of continuity for ions in the electrode sheath. The flux now includes a convective as well as a diffusive component:

$$\Gamma = D\frac{\partial n_p}{\partial x} + n_p \mu E, \tag{13}$$

where n_p is the positive ion density, μ is the ion mobility, which may be field-dependent, and E is the sheath electric field. When the field is large, the convective term, $n_p \mu E$ will dominate both the diffusive loss term and the homogeneous loss terms in Eq. 1.

Of course, the electric field is determined by the net charge density according to Poisson's equation:

$$\frac{\partial E}{\partial x} = \frac{e}{\epsilon_0}(n_p - n_n) \tag{14}$$

where e is the electronic charge, ϵ_0 is the permittivity of vacuum, and n_n is the negative charge density. Thus, Eqs. 13 and 14 need to be solved self-consistently (along with similar equations for electrons and negative ions) to obtain both the charge densities and the electric fields [10,11].

Experimentally, sheath fields can be measured non-intrusively by using a laser to excite parity-mixed rotational levels of polar diatomic molecules [4,5,9]. From the spectrally-resolved laser-induced fluorescence, relative intensities of nominally forbidden and allowed

transitions are used to determine the magnitude of the electric field with spatial resolution of 100-200 μm and temporal resolution of 10—20ns.

The data in Fig. 3 show how the fields vary in space and time during the first quarter of the cathodic half-cycle in a 50 kHz discharge through 95%Ar and 5%BCl_3. The BCl $A^1\Pi \leftarrow X^1\Sigma^+$ transition was used to determined the magnitudes of the field. Notice how the position of the plasma-sheath boundary expands as the applied voltage grows increasingly negative. The extraction of positive ions toward the electrode and the repulsion of electrons and negative ions toward the plasma results in charge depletion that permits the field to penetrate further into the plasma. This is apparent from the zero slope of the field near the electrode (see Eq. 14).

The extraction of ions by the low frequency field can also be seen by using LIF to measure ion densities [6]. During the positive part of the cycle, the ion density builds in the sheath because of electron-impact ionization. After the applied voltage reaches a maximum and becomes increasingly more negative, the ions are swept from the sheath. But, the time at which the ions are extracted depends on the distance from the electrode because of the finite time required for the sheath to expand (Fig. 3).

The periodic build-up and extraction of ions from the sheath distinguishes the low frequency discharge from both dc discharges and high frequency discharges. In the dc discharge, the cathodic field is time-independent and the ion density does not have a chance to build-up as in the anodic part of the low frequency cycle. In the high frequency sheath, ions cannot respond to the instantaneous field. Therefore, their density and energy are determined by the time-averaged component of the rf field, which is considerably smaller than the peak fields found in low frequency discharges. This is one reason *ion-enhanced* etching rates are lower in higher frequency plasmas [12].

VI. CONCLUSION

Three applications of space-time resolved spectroscopy to the study of plasma processes have been described.

Using time-averaged, spatially-resolved laser-induced fluorescence the concentrations of reactants near surfaces can be measured and the relative rates of reactions at those surfaces determined. Evidence was found for an enhanced loss rate for vibrationally hot CF_2 molecules at a Si surface and for ion-accelerated O atom etching of kapton in rf oxygen discharges.

From time-resolved measurements of emission intensities, slow and fast dissociative excitation mechanisms were distinguished in discharges containing Ar and BCl_3. Superelastic collisions of electrons with Ar metastables was found to be an important mechanism by which BCl excited states are formed. An order of magnitude enhancement in the BCl $A^1\Pi$ emission intensity results from this process when BCl_3 is diluted with Ar.

From space-time resolved electric field and ion density measurements, the mechanism for ion transport in a low frequency sheath was elucidated. As the voltage on the electrode grows increasingly negative, the sheath expands and extracts the ions toward the electrode. In this fashion, pulses of high energy ions impact surfaces and enhance the rates of heterogeneous reactions.

REFERENCES

[1] J.W. Thoman, K. Suzuki, S.H. Kable, and J.I. Steinfeld, J. Appl. Phys. **60**, 2775 (1986).

[2] G. Selwyn, J. Appl. Phys. **60**, 2771 (1986).

[3] G.R. Scheller, R.A. Gottscho, T. Intrator, and D.B. Graves, in preparation.

[4] C. A. Moore, G. P. Davis, and R. A. Gottscho, Phys. Rev. Lett. **52**, 538 (1984); M. L. Mandich, C. E. Gaebe, and R. A. Gottscho, J. Chem. Phys. **83**, 3349 (1985).

[5] R.A. Gottscho, Phys. Rev. A. (September 1987)

[6] R. A. Gottscho, R. H. Burton, D. L. Flamm, V. M. Donnelly, and G. P. Davis, J. Appl. Phys. **55**, 2707 (1984).

[7] D. K. Doughty and J. E. Lawler, Appl. Phys. Lett. **45**, 611 (1984).

[8] B.N. Ganguly and A. Garscadden, Appl. Phys. Lett. **46**, 540 (1985).

[9] J. Derouard and N. Sadeghi, Opt. Comm.**57**, 239 (1986).

[10] D.B. Graves and K.F. Jensen, IEEE Trans. Plasma Sci. **14**, 78 (1986).

[11] J.P. Boeuf, Phys. Rev. A (in press).

[12] R. H. Bruce, in *Plasma Processing*, R. G. Frieser and C. J. Mogab, eds., The Electrochemical Society (Pennington, NJ, 1981), p. 243.